Strain accumulation across the Coast Ranges at the latitude of San Francisco, 1994–2000

J. C. Savage, W. Gan,[1] W. H. Prescott,[2] and J. L. Svarc
U.S. Geological Survey, Menlo Park, California, USA

Received 4 June 2003; revised 5 December 2003; accepted 26 December 2003; published 30 March 2004.

[1] A 66-monument geodetic array spanning the Coast Ranges near San Francisco has been surveyed more than eight times by GPS between late 1993 and early 2001. The measured horizontal velocities of the monuments are well represented by uniform, right-lateral, simple shear parallel to N29°W. (The local strike of the San Andreas Fault is ~N34°W.) The observed areal dilatation rate of 6.9 ± 10.0 nstrain yr^{-1} (quoted uncertainty is one standard deviation and extension is reckoned positive) is not significantly different from zero, which implies that the observed strain accumulation could be released by strike-slip faulting alone. Our results are consistent with the slip rates assigned by the *Working Group on California Earthquake Probabilities* [2003] to the principal faults (San Gregorio, San Andreas, Hayward-Rodgers Creek, Calaveras-Concord-Green Valley, and Greenville Faults) cutting across the GPS array. The vector sum of those slip rates is 39.8 ± 2.6 mm yr^{-1} N29.8°W ± 2.8°, whereas the motion across the GPS array (breadth 120 km) inferred from the uniform strain rate approximation is 38.7 ± 1.2 mm yr^{-1} N29.0°W ± 0.9° right-lateral shear and 0.4 ± 0.9 mm yr^{-1} N61°E ± 0.9° extension. We interpret the near coincidence of these rates and the absence of significant accumulation of areal dilatation to imply that right-lateral slip on the principal faults can release the accumulating strain; major strain release on reverse faults subparallel to the San Andreas Fault within the Coast Ranges is not required. *INDEX TERMS:* 1206 Geodesy and Gravity: Crustal movements—interplate (8155); 1243 Geodesy and Gravity: Space geodetic surveys; 8150 Tectonophysics: Plate boundary—general (3040); *KEYWORDS:* strain accumulation, San Francisco, San Andreas Fault

Citation: Savage, J. C., W. Gan, W. H. Prescott, and J. L. Svarc (2004), Strain accumulation across the Coast Ranges at the latitude of San Francisco, 1994–2000, *J. Geophys. Res.*, *109*, B03413, doi:10.1029/2003JB002612.

1. Introduction

[2] The presence of young fold-and-thrust belts along and subparallel to the San Andreas Fault in central California [*Aydin*, 1982; *Page*, 1982; *Jones et al.*, 1994; *Page et al.*, 1998] suggests convergence normal to the fault. Although the geologic evidence for shortening associated with these fold-and-thrust belts is overwhelming, contemporary convergence across them has not been demonstrated geodetically. This is rather surprising considering the clear geodetic evidence for accumulation of shear strain along the San Andreas Fault. In this paper we examine recent Global Positioning System (GPS) surveys in the San Francisco Bay area in an attempt to detect the expected convergence normal to the San Andreas Fault system. We do not find it.

[3] We argue here that in the presence of a shear zone, simply showing contraction along a profile across the shear zone is not sufficient to demonstrate convergence. Such a profile across a zone of right-lateral, simple shear will show no contraction if the profile is oriented perpendicular to the direction of shear and extension (contraction) if the profile is oriented slightly clockwise (counterclockwise) from the perpendicular. Thus contraction along a profile could be observed in the absence of convergence if the profile is not strictly perpendicular to the shear. However, convergence involves consumption of surface area, and the measure of that consumption, areal dilatation, is a scalar. Thus detection of negative areal dilatation is diagnostic of convergence even where the precise orientation of the shear zone is not known. We argue that the observation of areal dilatation is critical to the demonstration of convergence.

[4] The deviatoric stress field averaged over the crustal thickness along the San Andreas Fault in central California is generally thought to consist of a large (~50 MPa) deviatoric compression normal to the fault (on the basis of the hypothesis that the crust is everywhere critically stressed, the coefficient of friction is 0.6, the pore pressure is hydrostatic [*Townend and Zoback*, 2000], and the observations that borehole breakouts in the Central Valley ~100 km east of San Francisco indicate that the principal compression axis is nearly normal the San Andreas Fault) and only a minor (<10 MPa) shear stress across it [*Zoback*

[1] Now at State Key Laboratory of Earthquake Dynamics, Institute of Geology, China Seismological Bureau, Beijing, China.
[2] Now at UNAVCO, Inc., Boulder, Colorado, USA.

et al., 1987; *Scholz*, 2000; *Zoback*, 2000]. That the deformation along the San Andreas Fault is dominated by right-lateral shear parallel to the fault is attributed to the weakness of the fault. However, during the interseismic interval when appreciable slip does not occur on the fault, one might expect to detect contraction normal to the fault in response to the large fault normal stress. On the basis of GPS surveys in southern California, *Feigl et al.* [1993] reported substantial convergence across the San Andreas Fault in the Carrizo Plain (~370 km southeast of San Francisco), but *Argus and Gordon* [2001] showed that this apparent convergence was an artifact of a faulty correction for slip on the San Andreas Fault. *Segall and Harris* [1986] used trilateration surveys to demonstrate fault normal convergence across the San Andreas Fault near Parkfield (~300 km southeast of San Francisco), but *Murray et al.* [2001], using GPS measurements, subsequently found no evidence for that fault normal convergence. Trilateration surveys across 100-km-wide zones spanning the San Andreas Fault failed to detect significant convergence across it in central California [*Lisowski et al.*, 1991]. *Savage et al.* [1998] found that neither significant contraction along a N58°E trend (perpendicular to the local Pacific plate motion relative to the Sierran plate) nor significant areal dilatation in the Coast Ranges near San Francisco was indicated by 1972–1989 trilateration surveys in the San Francisco Bay area. *Argus and Gordon* [2001] calculated the convergence across the San Andreas Fault system in central California on the basis of the assumption that the motion of the Pacific plate relative to the Sierran plate derived from space geodetic measurements was accommodated wholly on that fault system. They found that the convergence varied along the length of the San Andreas Fault in central California but was $<3.1 \pm 0.5$ mm yr^{-1}. Near San Francisco they found a convergence of -2.6 mm yr^{-1} (i.e., extension rather than contraction) over a short segment of the San Andreas Fault system. *Argus and Gordon* [2001] showed that the convergence that they inferred in central California acting over ~5 Myr could account for the present average elevation of the Coast Ranges. Convergence (3.8 ± 2.1 mm yr^{-1} according to *Prescott et al.* [2001] and 2.4 ± 0.4 mm yr^{-1} according to *Murray and Segall* [2001]) perpendicular to the local Pacific plate motion relative to North America (NA) has recently been reported at the east edge of the Coast Ranges in the San Francisco Bay region.

[5] Here we show that near San Francisco the velocity field across a 120-km-wide zone spanning the San Andreas Fault is well explained by uniform 161 ± 5 nstrain yr^{-1} right-lateral, simple shear parallel to N29°W ± 0.9°. The local strike of the San Andreas Fault is ~N34°W, and the local direction of motion of the Pacific plate relative to the Sierran plate is ~N32°W [*Argus and Gordon*, 2001] in this area. The measured areal dilatation rate within the zone is 7 ± 10 nstrain yr^{-1}. Because dip-slip faulting involves a change in surface area, the absence of significant areal dilatation suggests that only strike-slip faulting is required to release the accumulating strain.

[6] The following conventions are observed in this paper: Quoted uncertainties in the text and tables are standard deviations, but error bars and ellipses in the figures show 95% confidence intervals. Strain is reckoned positive in extension, and tensor, rather than engineering, shear strain rates are used. All velocities and rotations are measured with respect to a nominally fixed interior North America [*Savage et al.*, 2001b]. Rotation about a vertical axis is reckoned positive in the counterclockwise sense as viewed from above the Earth.

2. Data

[7] To study the deformation across the Coast Ranges near San Francisco, an array of geodetic monuments (triangles in Figure 1) in the region were surveyed more than eight times between late 1993 and early 2001with GPS. The individual monuments were occupied for at least 6 hours on 1 or more days in each survey. The data were reduced using point positioning [*Zumberge et al.*, 1997], GIPSY/OASIS-II software, release 6 [*Webb and Zumberge*, 1995], and satellite and clock files from the Jet Propulsion Laboratory. The phase ambiguities in each survey were resolved in the network processing mode. The data were then adjusted using the QOCA software [*Dong et al.*, 1998] (see also http://sideshow.jpl.nasa.gov/~dong/qoca/) subject to the constraint that the motion is linear in time over 1993–2001 interval. All velocities and rotations derived here are referred to a coordinate system in which interior North America (NA) is nominally fixed [*Savage et al.*, 2001b]. *Prescott et al.* [2001] previously discussed the measurements at the north end of this array, but our present discussion includes an additional year of data not available to them. (The observed velocities, the coordinates of the individual monuments, and the plots of position of each monument as a function of time can be found at http://quake.wr.usgs.gov/research/deformation/gps/qoca/SF_Bay_Area/.) The standard deviation for each component of horizontal velocity is ~1 mm yr^{-1}.

[8] The geodetic array shown in Figure 1 has been divided into five profiles, each trending roughly perpendicular to the San Andreas Fault. Plots of the velocity components parallel and perpendicular to the local direction of motion of the Pacific plate relative to NA (~N35°W) in the San Francisco area are shown in Figure 2. In profiles 4 and 5 (the southernmost profiles) the velocity distribution is discontinuous because of creep (continuous fault slip at the surface) on the San Andreas and Calaveras Faults. The velocity distributions are more uniform in profiles 1, 2, and 3, and we will approximate those velocity distributions by uniform strain. In what follows, we will be concerned only with profiles 1, 2, and 3, which we will refer to as the Bay array. The velocity field for the Bay array is shown in Figure 3.

[9] *Prescott et al.* [2001] and *Murray and Segall* [2001] reported a zone of N56°W contraction along the east edge of the Coast Ranges. (The Coast Ranges correspond to the area of topographic relief in Figure 3. The Central Valley is the adjacent area of no significant relief in the northeast corner of Figure 3.) The evidence for this zone of contraction is shown in Figure 4, which updates *Prescott et al.* [2001, Figure 5]. Figure 4 shows a velocity profile along a great circle passing through profile 1 and the Pacific-NA pole of rotation [*Argus and Gordon*, 2001]. The velocity components plotted for each monument are those parallel and perpendicular to that great circle. The data within the Coast Ranges segment of the profile are for monuments

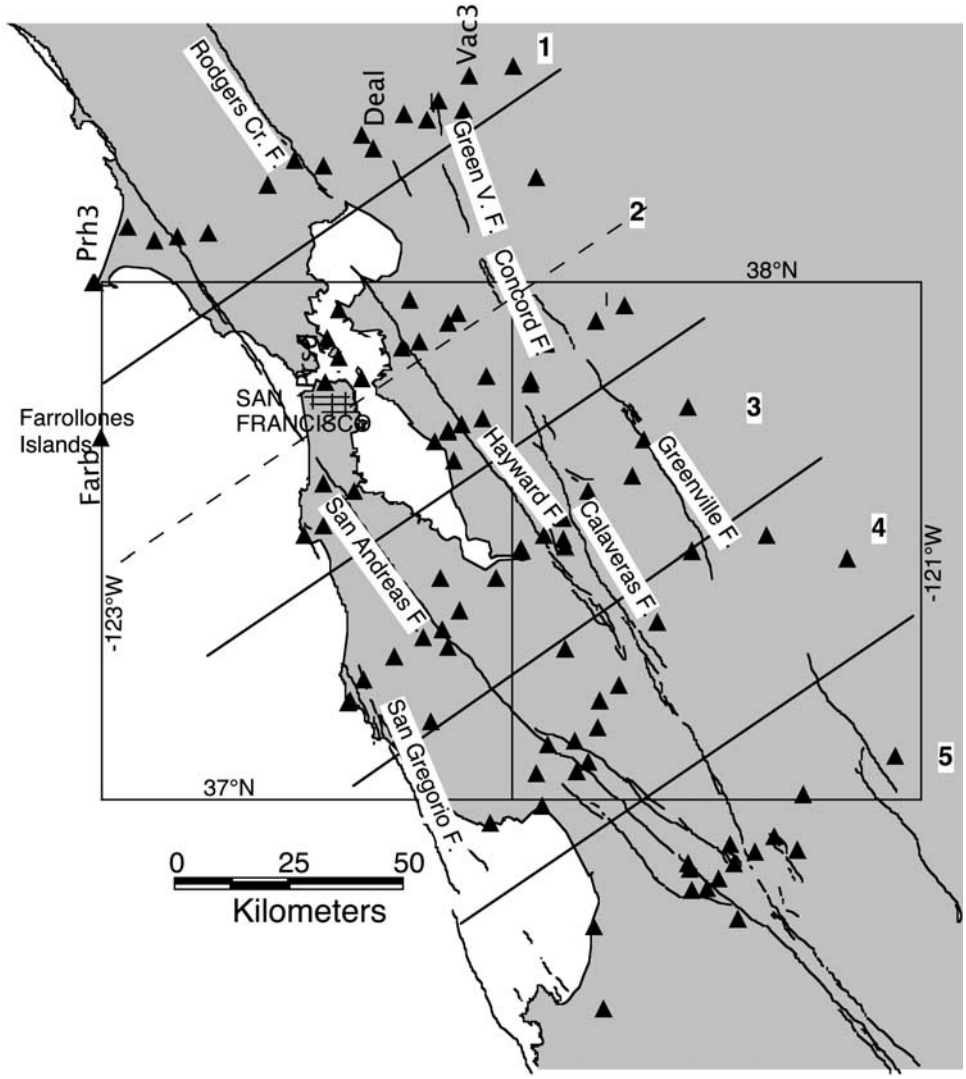

Figure 1. Map of San Francisco Bay area showing the locations of the geodetic monuments in the GPS array and the principal faults [*Jennings*, 1994]. The geodetic monuments have been grouped into northeast trending profiles indicated by numbers at the northeast end.

from profile 1 and the northern part of profile 2 (Figure 1). The data for monuments farther east (Central Valley and Sierra Nevada) are from the Bay Area Regional Deformation network of continuous GPS stations as used by *Prescott et al.* [2001]. (Notice that we have not included Ovro, the easternmost monument used by Prescott et al., as it is east of the Sierra Nevada block.) Figure 4 differs from Figure 5 of *Prescott et al.* [2001] in that the velocities were calculated from a longer run of data, which included data from 2000 and early 2001. The transverse component of velocity in Figure 4 shows the expected effect of the right-lateral San Andreas Fault system. Our interest here is in the great circle parallel component, which is directed ~N55°E. Whereas the earlier data [*Prescott et al.*, 2001, Figure 5] suggested an offset (see horizontal straight lines in Figure 4) in the velocity profile between monuments Deal and Vac3, the more recent data suggest a nearly uniform contraction between monuments Prh3 and Vac3. *Prescott et al.* [2001] interpreted the apparent offset in their data at the east end of the Coast Ranges as a narrow zone of contraction, whereas we interpret the new data to indicate a nearly uniform zone of contraction (inclined dashed line in Figure 4) across the breadth of the Coast Ranges. In neither interpretation is there significant deformation across the Central Valley and the Sierra Nevada (Figure 4).

[10] If the strain and rotation rates were uniform across the entire array, the velocity field could be described by [*Jaeger*, 1964, p. 39]

$$u = \varepsilon_{11}x + \varepsilon_{12}y - \omega y$$
$$v = \varepsilon_{12}x + \varepsilon_{22}y + \omega x, \quad (1)$$

where (x, y) and (u, v) are the coordinates and components of velocity relative to the centroid of the array, ε_{ij} is the (i, j) component of the strain rate tensor, and ω is the rotation rate about a vertical axis. A uniform strain and rotation rate approximation to the observed velocity field can be obtained by determining the values of ε_{ij} and ω in equation (1) that best fit the observed velocity field. We

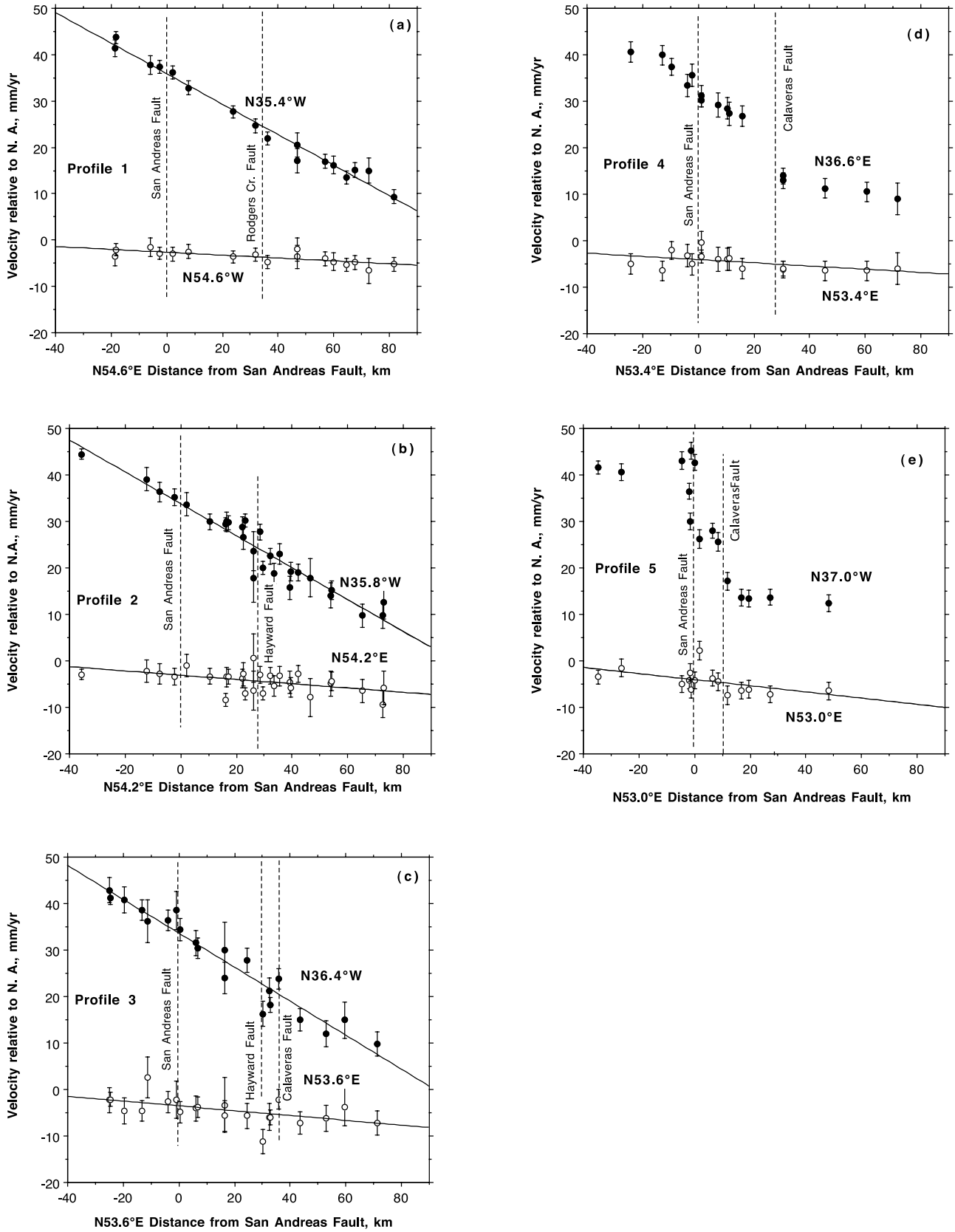

Figure 2. Velocities parallel (~N35°W) and perpendicular (~N55°E) to the local motion of the Pacific plate with respect to interior North America (NA) plotted as a function of distance from the San Andreas Fault for each of the profiles defined in Figure 1. The error bars represent 2 standard deviations on either side of the plotted point.

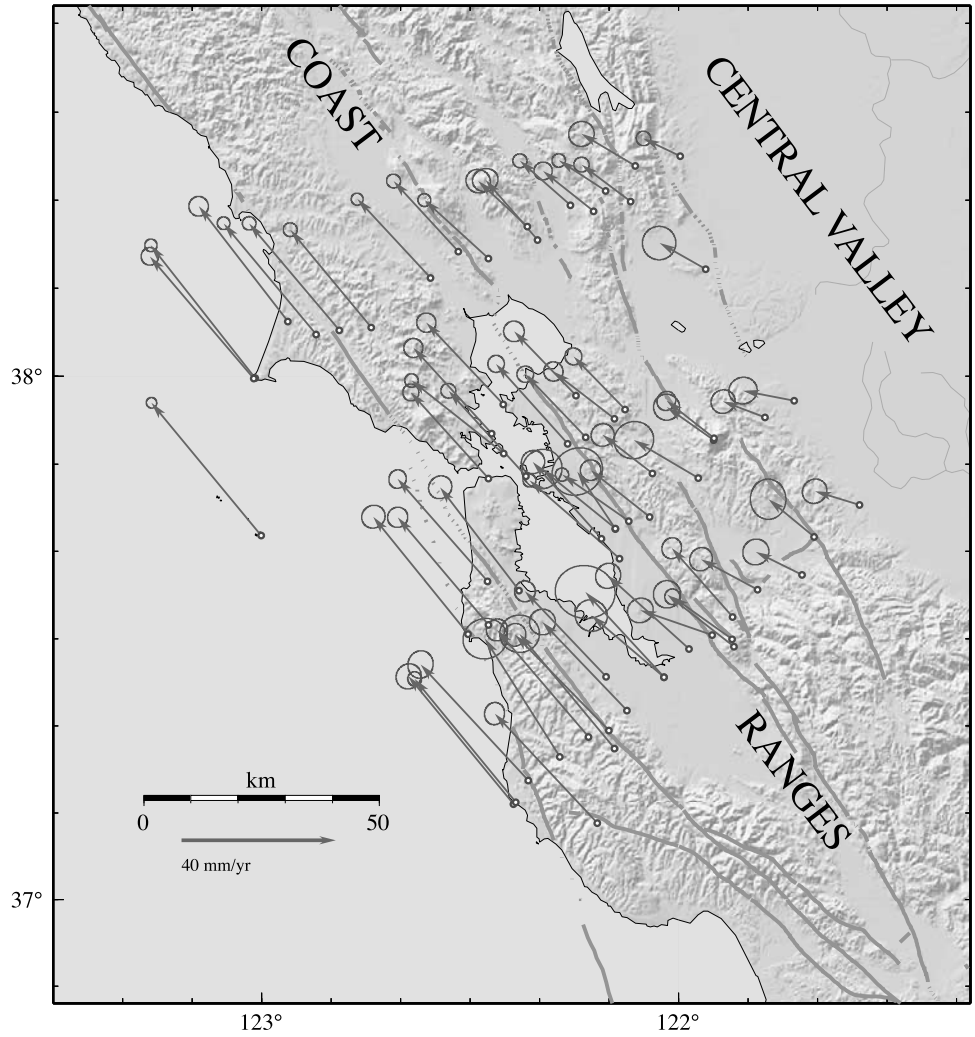

Figure 3. Velocities (arrows) inferred from repeated GPS surveys of the Bay array (profiles 1, 2, and 3 in Figure 1). The error ellipses at the ends of the arrows bound the 95% confidence regions. Velocities are measured with respect to nominally fixed North America. The mapped faults [*Jennings*, 1994] are shown by sinuous lines. See color version of this figure in the HTML.

have done this for the Bay array using the Earth-centered spherical coordinate equivalent of equation (1) [*Savage et al.*, 2001a]. The residuals, observed velocities less those predicted by this uniform strain and rotation rate approximation, are shown in Figure 5. The residuals appear to become larger as one goes from northwest to southeast, but in general, they are within the measurement errors as represented by the 95% confidence ellipses.

[11] The uniform strain and rotation rate approximation provides estimates of the average rate of deformation across the Bay array. The vertical axis rotation rate relative to fixed North America $\omega = -178.7 \pm 5.0$ nrad yr^{-1}, the dilatation rate 6.9 ± 10.0 nstrain yr^{-1}, and the orientation of the axis of maximum contraction rate N16.0°E ± 0.9°E for the best fit uniform strain and rotation rate approximation are independent of the orientation of the coordinate system chosen. The best fit uniform strain rate shown in Table 1 refers to coordinate systems with several different orientations. A Mohr circle representation of that strain rate tensor is shown in Figure 6. *Terzaghi* [1943, pp. 17–19] [see also *Mandl*, 1988, pp. 237–239] has shown that for uniform strain at a free surface (plane stress), there exists a point (the so-called pole) on the Mohr circle such that the strain rates across a vertical plane striking at azimuth θ measured clockwise from north are given by the opposite intersection with the Mohr circle of a line through that pole, making that same angle θ clockwise from the shear strain rate axis. In Figure 6 the pole is located by representing the vertical plane across which contraction is maximum on the Mohr circle. The N16°E plane in Table 1 strikes S74.0°E (106° clockwise from north), and the normal and shear strain rates across it are −157.9 and 0 nstrain yr^{-1}, respectively. The line representing that plane is then drawn through (−157.9, 0) the Mohr circle at an angle of 106.0° clockwise from the shear strain rate axis; the opposite intersection of that line with the Mohr circle is the desired pole (Figure 6). A line drawn through that pole making an angle θ clockwise from the shear strain rate axis will represent a vertical plane striking at azimuth θ, and the intersection opposite to the pole of that line with the Mohr circle will give the strain rates across the plane. For example, in Figure 6 one can see that the vertical plane across which normal extension is zero

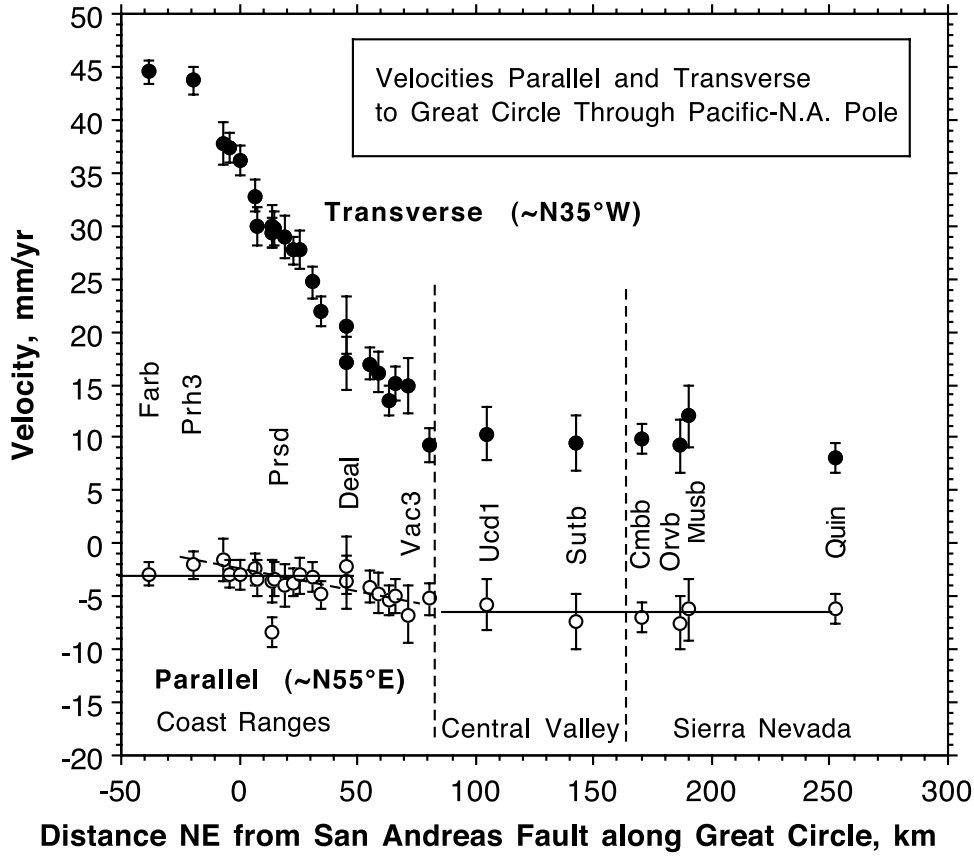

Figure 4. Velocity profile along a great circle passing through profile 1 and the Pacific-NA pole of rotation. The velocity components shown are those parallel and transverse to the great circle passing through the monument and the Pacific-NA pole of rotation. The error bars represent 2 standard deviations on either side of the plotted point. Names of some of the monuments are shown for comparison with *Prescott et al.* [2001, Figure 5]; the locations of those monuments in the Coast Ranges are shown in Figure 1.

strikes N29.6°W. Figure 6 shows that for planes striking near N30°W the extension across the plane is near zero and that small changes in azimuth determine whether contraction or extension obtains across the plane.

[12] The uniform strain and rotation rate fits to various subsets of the Bay array are shown in Table 2. Table 2 shows the fit to all data and the selected values show the fit when with the five monuments contributing the largest residuals to the fit for all data are removed. In addition, we have divided the Bay array into four subarrays and found the uniform strain and rotation rates that best approximate the velocities observed in each subarray (Table 2). The NW/2 (29 monuments) and SE/2 (37 monuments) subarrays consist of monuments in the Bay array northwest and southeast, respectively, of a line (dashed line in Figure 1) trending N56°E through San Francisco. The NE/2 (30 monuments) and SW/2 (36 monuments) subarrays consist of the monuments in the Bay array northeast and southwest, respectively, of the Hayward-Rodgers Creek Fault (Figure 1). The uniform strain rates in Table 2 refer to a coordinate system with the 1 axis directed N61°E and the 2 axis directed N29°W. The areal dilatation rate Δ, azimuth of the principal contraction rate axis, and rotation rate ω are independent of the reference coordinate system. Those quantities for the subarrays are compared with those found for the entire Bay array in Table 2. Although there are differences between the entire array and the individual subarrays in these strain and rotation rates, the quantities are generally consistent. The azimuth of the maximum contraction rate axis is particularly stable.

[13] The simplest interpretation of the uniform strain rate approximation is given in a coordinate system with the 1 axis directed N61°E and the 2 axis directed N29°W. Then strain accumulation across the Coast Ranges near San Francisco Bay is given by N29.0°W values in Table 1. There the extension rates ε_{11} and ε_{22} are not significantly different from zero, and the shear strain rate $\varepsilon_{12} = -161.3 \pm 5.0$ nstrain yr^{-1} is only marginally different from the rotation rate $\omega = -178.5 \pm 5.0$ nrad yr^{-1}. Thus the motion relative to fixed North America is approximated by right-lateral, simple ($\omega = \varepsilon_{12}$) shear parallel to N29°W. The N61°E dimension of the Bay array is w = 120 km. Then the relative motion across the Coast Ranges implied by that strain rate is $2\varepsilon_{12}w = 38.7 \pm 1.2$ mm yr^{-1} N29.0°W right-lateral shear and $\varepsilon_{11}w = 0.4 \pm 0.9$ mm yr^{-1} N61.0°E extension.

3. Discussion

[14] The Working Group on California Earthquake Prediction (WGCEP) has estimated the secular slip rates on the principal faults in the San Francisco Bay area [*Working*

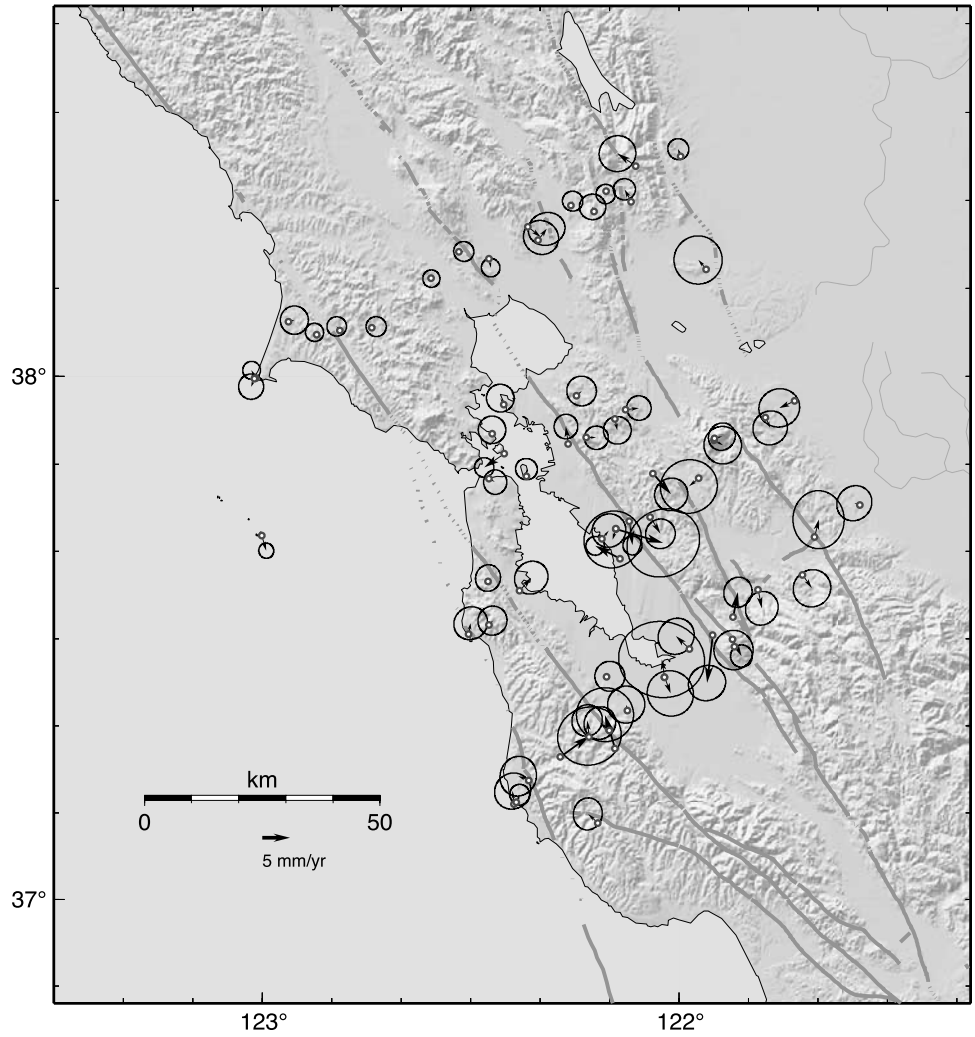

Figure 5. Residuals (arrows) from the uniform strain rate fit to the velocity data for the Bay array (profiles 1, 2, and 3 in Figure 1). The error ellipses at the end of the arrows bound the 95% confidence regions. The mapped faults [*Jennings*, 1994] are shown by sinuous lines.

Group on California Earthquake Probabilities, 2003, Table 3.8]. Those slip rates were based primarily on observations of offset geological or cultural features and represent averages over intervals from hundreds to several tens of thousands of years. Some of those principal faults appear to be simply continuations of other principal faults, and in those cases we have joined them to form a single throughgoing fault. For example, the Rodgers Creek Fault appears to be the northward extension of the Hayward Fault (Figure 1), and we have combined the two into the Hayward-Rodgers Creek Fault. Similarly, we have combined the Calaveras, Concord, and Green Valley Faults (Figure 1) into the Calaveras-Concord-Green Valley Fault. The WGCEP slip rates for these principal faults are shown in Table 3. To designate an average strike for each of those faults, we have approximated the fault trace across the Bay array by a straight line (Figure 7), and the strikes of those linear approximations are listed in Table 3. Because the faults are assumed to be throughgoing, the secular relative motion across the Bay array due to them should be given by the sum of the slip rate vectors (slip rate at azimuth of fault strike) in Table 3. That vector sum is 39.8 ± 2.6 mm yr^{-1} N29.8°W ± 2.8°. This treatment may not be completely proper for the Greenville and San Gregorio Faults, both of which have been continued northwestward in Figure 7 beyond their mapped lengths. If the Greenville Fault were not included in the vector sum, the relative motion would be 37.8 ± 2.5 mm yr^{-1} N29.5°W ± 2.8°, not a significant change. If the San Gregorio Fault were not included in the vector sum, the relative motion would be 32.9 ± 2.2 mm yr^{-1} N31.7°W ± 3.1°. Because that value is significantly less in magnitude than the relative motion (38.7 mm yr^{-1}) actually measured across the Bay array, we argue that the San Gregorio Fault should be included in the vector sum. Then the WGCEP estimates imply that the principal faults in the Coast Ranges near San Francisco are accumulating a slip deficit at a rate (39.8 ± 2.6 mm yr^{-1} N29.8°W ± 2.8°) nearly identical to the relative motion (38.7 ± 1.2 mm yr^{-1} N29.0°W ± 0.9°) across the Coast Ranges inferred from the uniform strain rate analysis. This coincidence suggests that the observed strain accumulation will eventually be released by seismic slip on the principal faults. That is, the observed strain accumulation is consistent with the strain release proposed by the WGCEP.

Table 1. Strain Rates for Various Coordinate Orientations

2 Axis Direction[a]	ε_{11}, nstrain yr^{-1}	ε_{12}, nstrain yr^{-1}	ε_{22}, nstrain yr^{-1}
N16.0°E	164.7 ± 7.2	0.0 ± 5.0	−157.9 ±6.9
N00.0°E	140.3 ± 7.7	−85.4 ± 5.0	−133.4 ± 6.4
N28.4°W	6.9 ± 7.9	−161.3 ± 5.0	0.0 ± 6.1
N29.0°W	3.6 ± 7.9	−161.3 ± 5.0	3.3 ± 6.1
N29.6°W	0.0 ± 7.9	−161.3 ± 5.0	6.9 ± 6.1
N32.0°W	−13.3 ± 7.9	−160.4 ± 5.0	20.2 ± 6.1
N34.2°W	−25.6 ± 7.8	−158.7 ± 5.0	32.5 ± 6.2

[a]The 1 axis is oriented 90° clockwise from the 2 axis.

[15] The observed strain accumulation may simply be a consequence of deep slip on the principal faults. The conventional model of strain accumulation [*Savage and Burford*, 1973] attributes the surface deformation near a fault to continuous slip below the locking depth (∼10 km) at the secular slip rate. Then the relative motion at the surface calculated by integrating the strain rate across a broad zone centered on the fault should equal the slip rate at which the fault slips at depth. That is, in the conventional model of strain accumulation the relative motion of distant points on either side of the fault is equal to the deep slip rate on the fault. Thus the conventional model predicts that the relative velocity accommodated across the Coast Ranges should be equal to the vector sum of the secular slip rates on the principal faults in the Coast Ranges, as observed.

[16] Although each is based on entirely different data, the strain rate fields for the San Francisco area determined in this paper, by *Savage et al.* [1998], and by *Argus and Gordon* [2001] are reasonably consistent. In a coordinate system with the 1 axis directed N58°E and the 2 axis directed N32°W we find from the 1994–2001 GPS data that $\varepsilon_{11} = -13.3 \pm 7.9$, $\varepsilon_{12} = -160.4 \pm 5.0$, and $\varepsilon_{22} = 20.2 \pm 6.1$ nstrain yr^{-1} (N32.0°W in Table 1); *Savage et al.* [1998] found from the 1972–1989 trilateration data that $\varepsilon_{11} = 9.2 \pm 7.4$, $\varepsilon_{12} = -160.7 \pm 4.6$, and $\varepsilon_{22} = 8.2 \pm 6.2$ nstrain yr^{-1}; and in the model of *Argus and Gordon* [2001] (Pacific plate moving N32°W relative to the Sierran plate at San Francisco), though specific strain rates are not given, only ε_{12} would be nonzero. The values found for ε_{11} in this paper and by *Savage et al.* [1998] differ by a marginally significant amount (22.5 ± 10.8 nstrain yr^{-1}), but the two estimates do not apply to exactly the same area. (The estimate of *Savage et al.* [1998] applies to an area equivalent to essentially the full array in Figure 1, whereas our estimate applies only to profiles 1, 2, and 3.) The orientation of the vertical plane subject to maximum right-lateral shear strain found in this paper is N29.0°W ± 0.9°, whereas the orientation found by *Argus and Gordon* [2001] is N32.4°W ± 0.7° at the location of San Francisco. The marginally significant difference (3.4° ± 1.1°) might be explained by internal deformation in the Sierran or Pacific

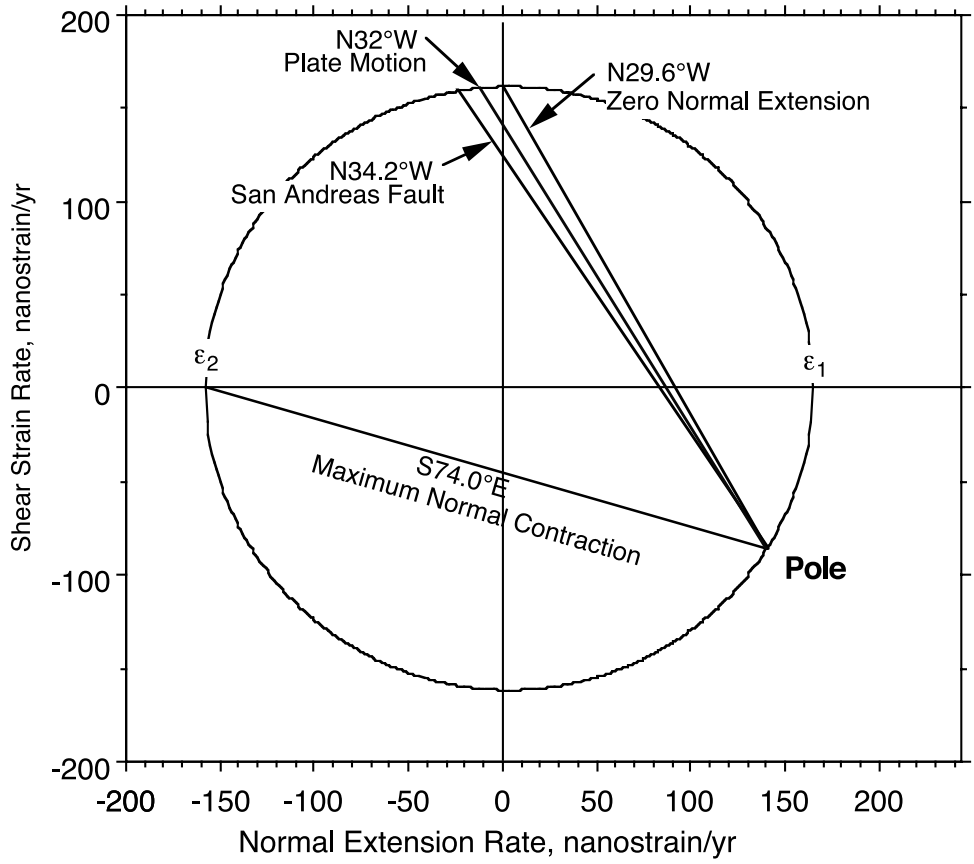

Figure 6. Mohr circle representation of the strain rate found as the best fit to the velocity data for the Bay array (profiles 1, 2, and 3 in Figure 1). A line drawn through the pole making an angle θ with the shear strain rate axis intersects the Mohr circle at a point representing the normal and shear strain rates across a vertical plane striking at the same angle with respect to north.

Table 2. Strain Rates for Various Subarrays With 1 Axis Directed N61°E and 2 Axis N29°W

Subarray	ε_{11}, nstrain yr^{-1}	ε_{12}, nstrain yr^{-1}	ε_{22}, nstrain yr^{-1}	$\Delta = \varepsilon_{11} + \varepsilon_{22}$, nstrain yr^{-1}	Azimuth Contraction, deg	Ω, nrad yr^{-1}
All	3.6 ± 7.9	−161.3 ± 5.0	3.3 ± 6.1	6.9 ± 10.0	N16.0°E ± 0.9°	−178.7 ± 5.0
Selected[a]	2.8 ± 6.5	−162.2 ± 4.2	5.3 ± 5.2	8.0 ± 8.3	N16.2°E ± 0.7°	−177.7 ± 4.1
NW/2	10.7 ± 8.1	−152.4 ± 7.8	15.7 ± 13.4	26.4 ± 15.7	N16.5°E ± 1.5°	−171.6 ± 7.8
SE/2	−14.0 ± 16.6	−177.2 ± 14.5	−15.2 ± 23.4	−29.3 ± 28.8	N15.9°E ± 2.3°	−197.4 ± 14.4
NE/2	−4.3 ± 21.8	−120.3 ± 11.8	22.8 ± 9.1	18.5 ± 23.6	N19.2°E ± 2.8°	−142.3 ± 11.8
SW/2	−2.0 ± 13.5	−146.2 ± 7.5	−12.1 ± 6.8	−14.1 ± 15.1	N15.0°E ± 1.5°	−161.6 ± 7.5

[a]The five monuments (Ante, Sher, Wint, Ebbb, Roc2, and Pbl1) with the largest residuals omitted.

plate. Recall that *Argus and Gordon* [2001, p. 1582] did not use velocities measured in the Coast Ranges in their calculation of the Sierran-Pacific motion but rather depended upon velocities measured in the interior of the Sierran and Pacific plates.

[17] We have suggested that the areal dilatation rate $\Delta = \varepsilon_{11} + \varepsilon_{22}$ is diagnostic in identifying convergence. That is, convergence requires $\Delta < 0$. Our observed value of $\Delta = 7 \pm 10$ nstrain yr^{-1} suggests a 95% probability that $\Delta > -10$ nstrain yr^{-1} and a 75% probability that $\Delta > 0$ (one-sided confidence intervals). The data of *Savage et al.* [1998] for trilateration surveys from 1972 to 1989 over an area similar to that covered by the Bay array (omit their polygons S1 through S4) indicate $\Delta = 36 \pm 10$ nstrain yr^{-1}, a value only marginally consistent with ours. F. F. Pollitz, and M. C. J. Nyst (A proposed physical model for strain accumulation in the San Francisco Bay region, submitted to *Geophysical Journal International*, 2003, Figure 6B) have analyzed almost the same GPS data that we used here and estimated the distribution of volumetric dilatation at the surface. Their values of the volumetric dilatation rate vary from −100 to 100 nstrain yr^{-1} over the area of the Bay array, but the average volumetric dilatation rate is -10.0 ± 7.8 nstrain yr^{-1} (M. C. J. Nyst, personal communication, 2003). At the free surface the volumetric dilatation should be about 2/3 of the areal dilatation Δ, which would imply an average areal dilatation rate of -15 ± 12 nstrain yr^{-1} in the Bay array. The difference (22 ± 16 nstrain yr^{-1}) between the estimate of areal dilatation by Pollitz and Nyst and our own estimate is not significant. Both estimates are consistent with a null dilatation rate, but their estimate favors a negative dilatation rate, whereas ours favors a positive rate. There is agreement that Δ is small compared with the shear strain rate.

[18] Elsewhere in central California, fold-and-thrust belts subparallel to the San Andreas Fault seem to require fault normal compression [*Zoback et al.*, 1987]. *Miller* [1998] has suggested that these folds may have originated as drag folds and then been rotated 20°–30° clockwise in the existing right-lateral shear field to their present orientation, in which orientation they have continued to grow because of compression normal to the San Andreas Fault. *Jones et al.* [1994] argue for folds and thrusts subparallel to the San Andreas in the Coast Ranges at the latitude of San Francisco. However, *Unruh and Lettis* [1998] find that the folds and thrusts in the Coast Ranges east of San Francisco are oriented obliquely with respect to the San Andreas Fault system, an orientation consistent with drag folding in a shear field subparallel to the principal strike-slip faults. The uniform strain rate field proposed here implies contraction across vertical planes striking parallel to the San Andreas Fault (Figure 6) and even greater contraction across planes striking more westerly, and this is consistent with thrust faulting and folding subparallel to the San Andreas Fault. However, the strain field does imply extension across vertical planes striking east of N29.6°W (e.g., the Calaveras or San Gregorio Faults). Moreover, our measurement precision does not allow us to exclude a small amount of N61°E convergence. For example, the observed areal dilatation of 0.7 ± 1.0 nstrain yr^{-1} would admit up to 1.2 mm yr^{-1} of N61°E convergence across the Bay array at the 95% confidence level.

[19] If the axis of maximum horizontal compression is almost normal to the San Andreas Fault [*Zoback et al.*, 1987], it is surprising that so little contraction is observed normal to the fault. The conventional explanation of strain accumulation across a throughgoing fault is that the upper portion of the fault is locked but the deeper portion, driven by the tectonic stress field, slips uniformly at its secular slip rate [*Savage and Burford*, 1973]. The deeper portions of the reverse faults subparallel to the San Andreas Fault in the Coast Ranges [*Page*, 1982; *Aydin*, 1982; *Jones et al.*, 1994; *Page et al.*, 1998] might then slip continuously, leading to a zone of contraction across the surface trace of the fault. If the axis of maximum compression is directed roughly normal to the San Andreas Fault [*Zoback et al.*, 1987] and the observed interseismic deformation is primarily shear subparallel to the San Andreas Fault, the absence of fault normal contraction within the Coast Ranges suggests that deep slip on reverse faults is somehow inhibited, whereas deep slip on strike−slip faults is facilitated. Then the measured strain rate field and tectonic stress field need not be proportional or even coaxial (i.e., principal strain rate axes need not be parallel to the principal stress axes).

[20] Despite our conclusion that major strain release on reverse faults subparallel to the San Andreas Fault within the area covered by the Bay array is not required by the observed strain accumulation rates, we concede that strain release on reverse faults outside of that area may be required. For example, reverse ruptures such as the 1989 Loma Prieta earthquake [*U.S. Geological Survey Staff*, 1990], which occurred near the crossing of profile 4 with the San Andreas Fault (Figure 1), may be expected along restraining bends in the San Andreas Fault system. In fact, because our measurements are not precise enough to ex-

Table 3. Right-Lateral, Secular Slip Rates and Approximate Strikes of the Principal Faults Across the Bay Array[a]

Fault	Slip Rate, mm yr^{-1}	Strike
San Gregorio	7 ± 1.5	N21°W
San Andreas	17 ± 2.0	N34°W
Hayward-Rodgers Creek	9 ± 1	N33°W
Calaveras-Concord-Green Valley	5 ± 1.5	N20°W
Greenville	2 ± 1	N35°W

[a]*Working Group on California Earthquake Probabilities* [2003, Table 3.8].

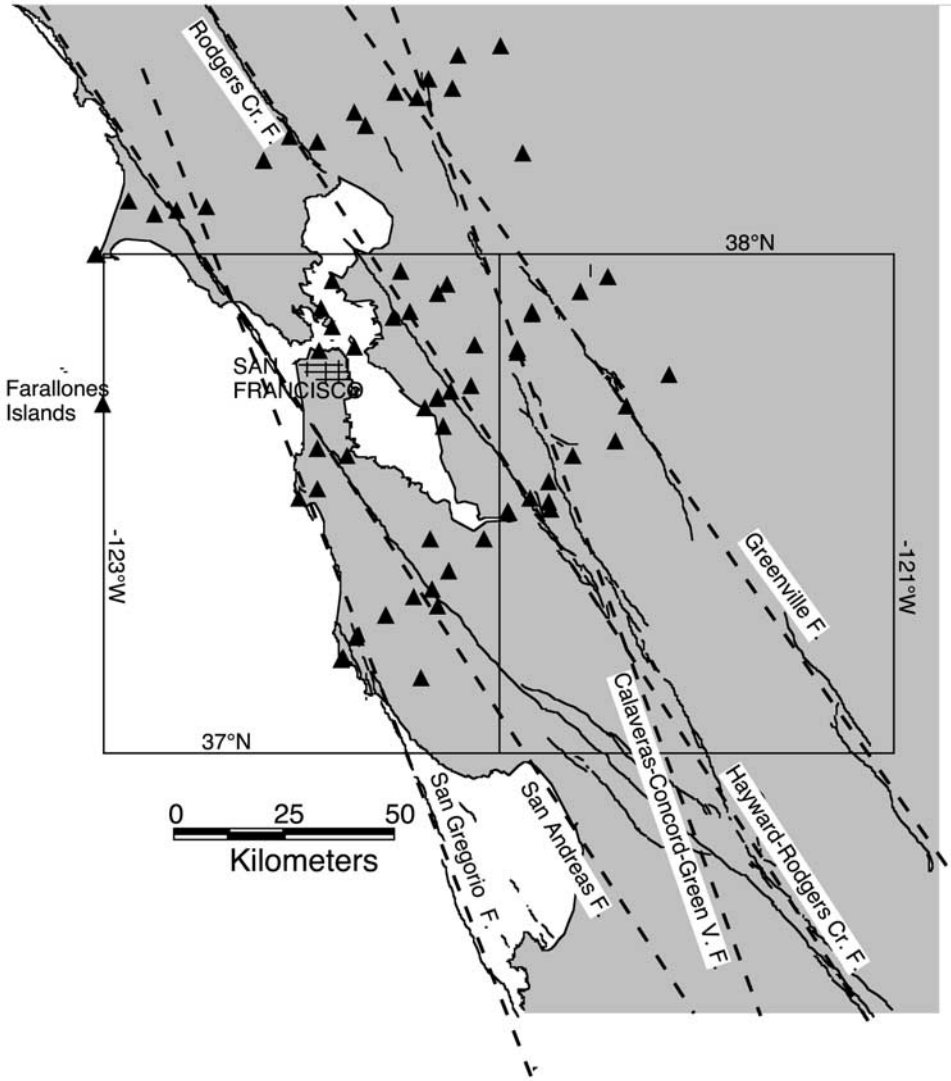

Figure 7. Linear approximations (heavy dashed lines) to the principal faults in the San Francisco Bay region. These representations are intended only to fit the faults in the area spanned by the Bay array (triangles).

clude contraction as large as 1 mm yr^{-1} at the 95% confidence level, infrequent strain release on reverse faults within the Bay array is not excluded.

[21] *Unruh and Lettis* [1998, Figure 2] analyzed earthquake focal mechanisms from the 1967–1996 interval in the San Francisco Bay region. They found that the orientation of the principal strain rate axes (their maximum incremental strain axes) northeast of the Hayward Fault was rotated 20°–30° clockwise from that southwest of the fault. Comparison of the orientation (Table 2) of the contraction axis for the NE/2 subarray (monuments northeast of the Hayward-Rodgers Creek Fault) with that of the SW/2 subarray (monuments southwest of the Hayward-Rodgers Creek Fault) shows that the former is only 4.2° ± 3.2° clockwise from the latter. However, Unruh and Lettis actually measured the orientation of the strain release axes (i.e., strain decrements associated with earthquakes), whereas we measure the orientation of the strain accumulation axes. The strain release principal axes are generally thought to be on the average coaxial with the principal stress axes. Then the orientation of the contraction axis found by Unruh and Lettis would generally be interpreted as the orientation of the principal compression axis. The principal axes of the strain rate tensor and the stress tensor need not be coaxial (e.g., in the presence of a background stress not coaxial with the present stress rate), and thus our observation of the principal contraction axis need not be consistent with the orientations of the principal compression axis of *Unruh and Lettis* [1998].

4. Conclusions

[22] The deformation across the Coast Ranges near San Francisco is remarkably uniform in space (see profiles 1, 2, and 3 in Figure 2), and the velocity field observed there may be approximated by a uniform strain and rotation rate (see residuals from that fit in Figure 5). The strain accumulation rate across the Coast Ranges near San Francisco is approximated by 161.3 ± 5.0 nstrain yr^{-1} uniform, right-lateral, simple shear across a vertical plane striking N29.0°W ±

0.9°. The strike of the San Andreas Fault in this area is N34°W. Thus there appears to be 25.6 ± 7.8 nstrain yr^{-1} (3.1 ± 0.9 mm yr^{-1} across the breadth of the Coast Ranges) contraction normal to the San Andreas Fault proper (N34°W in Table 1). However, the San Andreas Fault system near San Francisco is made up of several fault strands (San Gregorio, San Andreas, Hayward-Rodgers Creek, Calaveras-Concord-Green Valley, and Greenville Faults), all of which are right lateral. The weighted (by secular slip rate; see Table 3) mean fault strike is N29.8°W ± 2.8°. Our uniform strain rate approximation (Figure 6) indicates a contraction across a vertical plane striking N29.8°W of −0.9 ± 7.9 nstrain yr^{-1} (−0.1 ± 0.9 mm yr^{-1} contraction across the Coast Ranges). Thus we detect no significant contraction across the San Andreas Fault system in the Coast Ranges near San Francisco. Moreover, the areal dilatation rate in the uniform strain and rotation rate approximation is an insignificant 6.9 ± 10.0 nstrain yr^{-1}, which implies that the observed strain accumulation can be released by strike-slip faulting alone. Indeed, the relative motion (38.7 ± 1.2 mm yr^{-1} N29.0°W ± 2.8) across the Coast Ranges inferred from the rate of strain accumulation is essentially the same as the total slip deficit accumulation (39.8 ± 2.6 mm yr^{-1} N29.8°W ± 2.8°) on the principal strike-slip faults in the Coast Ranges near San Francisco as estimated by the *Working Group on California Earthquake Probabilities* [2003, Table 3.8].

[23] **Acknowledgment.** This paper was improved by incorporating suggestions from Robert W. Simpson.

References

Argus, D. F., and R. G. Gordon (2001), Present tectonic motion across the Coast Ranges and San Andreas Fault system in central California, *Geol. Soc. Am. Bull.*, *113*, 1580–1592.

Aydin, A. (1982), The East Bay hills, a compressional domain resulting from interaction between the Calaveras and Hayward-Rodgers Creek Faults, in *Proceedings of Conference on Earthquake Hazards in the Eastern San Francisco Bay Area*, edited by E. W. Hart, S. E. Hirschfeld, and S. S. Schulz, *Spec. Publ. Calif. Div. Mines Geol.*, *62*, 11–21.

Dong, D., T. A. Herring, and R. W. King (1998), Estimating regional deformation from a combination of space and terrestrial geodetic data, *J. Geod.*, *72*, 200–214.

Feigl, K. L., et al. (1993), Space geodetic measurement of the velocity field of central and southern California, 1984–1992, *J. Geophys. Res.*, *98*, 21,677–21,712.

Jaeger, J. C. (1964), *Elasticity, Fracture and Flow*, corrected 2nd ed., 212 pp., Methuen, New York.

Jennings, C. W. (1994), Fault activity map of California and adjacent areas, *Geol. Data Map 6*, Calif. Dep. of Conserv., Div. of Mines and Geol., Sacramento.

Jones, D. L., R. Graymer, C. Wang, T. V. McEvilly, and A. Lomax (1994), Neogene transpressive evolution of the California Coast Ranges, *Tectonics*, *13*, 561–574.

Lisowski, M., J. C. Savage, and W. H. Prescott (1991), The velocity field along the San Andreas Fault in central and southern California, *J. Geophys. Res.*, *96*, 8369–8389.

Mandl, G. (1988), *Mechanics of Tectonic Faulting*, Elsevier Sci., New York.

Miller, D. D. (1998), Distributed shear, rotation and partitioned strain along the San Andreas Fault, central California, *Geology*, *26*, 867–870.

Murray, J. R., P. Segall, P. Cervelli, W. Prescott, and J. Svarc (2001), Inversion of GPS data for spatially variable slip-rate on the San Andreas Fault near Parkfield, CA, *Geophys. Res. Lett.*, *28*, 359–362.

Murray, M. H., and P. Segall (2001), Modeling broadscale deformation in northern California and Nevada from plate motions and elastic strain accumulation, *Geophys. Res. Lett.*, *28*, 4315–4318.

Page, B. M. (1982), Modes of Quaternary tectonic movement in the San Francisco Bay region, California, in *Proceedings of Conference on Earthquake Hazards in the Eastern San Francisco Bay Area*, edited by E. W. Hart, S. E. Hirschfeld, and S. S. Schulz, *Spec. Publ. Calif. Div. Mines Geol.*, *62*, 1–10.

Page, B. M., G. A. Thompson, and R. G. Coleman (1998), Late Cenozoic tectonics of the central and southern Coast Ranges of California, *Geol. Soc. Am. Bull.*, *110*, 846–876.

Prescott, W. H., J. C. Savage, J. L. Svarc, and D. Manaker (2001), Deformation across the Pacific-North America plate boundary near San Francisco, California, *J. Geophys. Res.*, *106*, 6673–6682.

Savage, J. C., and R. O. Burford (1973), Geodetic determination of relative plate motion in central California, *J. Geophys. Res.*, *78*, 832–845.

Savage, J. C., R. W. Simpson, and M. H. Murray (1998), Strain accumulation rates in the San Francisco Bay area, 1972–1989, *J. Geophys. Res.*, *103*, 18,039–18,051.

Savage, J. C., W. Gan, and J. L. Svarc (2001a), Strain accumulation and rotation in the Eastern California Shear Zone, *J. Geophys. Res.*, *106*, 21,995–22,007.

Savage, J. C., J. L. Svarc, and W. H. Prescott (2001b), Strain accumulation near Yucca Mountain, Nevada, 1993–1998, *J. Geophys. Res.*, *106*, 16,483–16,488.

Scholz, C. H. (2000), Evidence for a strong San Andreas Fault, *Geology*, *28*, 163–166.

Segall, P., and R. Harris (1986), Slip deficit on the San Andreas Fault at Parkfield, California, as revealed by the inversion of geodetic data, *Science*, *233*, 1409–1413.

Terzaghi, K. (1943), *Theoretical Soil Mechanics*, John Wiley, Hoboken, N. J.

Townend, J., and M. D. Zoback (2000), How faulting keeps the crust strong, *Geology*, *28*, 399–402.

Unruh, J. R., and W. R. Lettis (1998), Kinematics of transpressional deformation in the eastern San Francisco Bay region, California, *Geology*, *26*, 19–22.

U.S. Geological Survey Staff (1990), The Loma Prieta, California, earthquake: An anticipated event, *Science*, *247*, 286–293.

Webb, F. H., and J. F. Zumberge (1995), An introduction to GIPSY/OASIS-II, JPL D-11088, Jet Propul. Lab., Calif. Inst. of Technol., Pasadena, Calif.

Working Group on California Earthquake Probabilities (2003), Earthquake probabilities in the San Francisco Bay region: 2002–2031, *U.S. Geol. Surv. Open File Rep., 03-214*. (available at http://geopubs.wr.usgs.gov/open-file/of03-214)

Zoback, M. L. (2000), Strength of the San Andreas, *Nature*, *405*, 31–32.

Zoback, M. D., et al. (1987), New evidence on the state of stress of the San Andreas Fault system, *Science*, *238*, 1105–1111.

Zumberge, J. F., M. B. Heflin, D. C. Jefferson, M. M. Watkins, and F. H. Webb (1997), Precise point positioning for the efficient and robust analysis of GPS data from large networks, *J. Geophys. Res.*, *102*, 5005–5017.

W. Gan, State Key Laboratory of Earthquake Dynamics, Institute of Geology, China Seismological Bureau, Beijing, China. (wjgan@gps.gov.cn)

W. H. Prescott, UNAVCO, Inc., 3360 Mitchell Lane, Suite C, Boulder, CO 80301-2245, USA. (prescott@unavco.org)

J. C. Savage and J. L. Svarc, U.S. Geological Survey, 345 Middlefield Dr., Menlo Park, CA 94025, USA. (jasavage@usgs.gov; jsvarc@usgs.gov)